Default mode network abnormalities in idiopathic generalized epilepsy

Megan L. McGill [a], Orrin Devinsky [a], Clare Kelly [b], Michael Milham [b], F. Xavier Castellanos [b], Brian T. Quinn [a], Jonathan DuBois [a], Jonathan R. Young [a], Chad Carlson [a], Jacqueline French [a], Ruben Kuzniecky [a], Eric Halgren [c], Thomas Thesen [a,c,*]

[a] NYU Comprehensive Epilepsy Center, New York University School of Medicine, New York, NY, USA
[b] Phyllis Green and Randolph Cowen Institute for Pediatric Neuroscience at the NYU Langone Medical Center, New York, NY, USA
[c] Multimodal Imaging Laboratory, University of California-San Diego, San Diego, CA, USA

ARTICLE INFO

ABSTRACT

Idiopathic generalized epilepsy (IGE) is associated with widespread cortical network abnormalities on electroencephalography. Resting state functional connectivity (RSFC), based on fMRI, can assess the brain's global functional organization and its disruption in clinical conditions. We compared RSFC associated with the 'default mode network' (DMN) between people with IGE and healthy controls. Strength of functional connectivity within the DMN associated with seeds in the posterior cingulate cortex (PCC) and medial prefrontal cortices (MPFC) was compared between people with IGE and healthy controls and was correlated with seizure duration, age of seizure onset and age at scan. Those with IGE showed markedly reduced functional network connectivity between anterior and posterior cortical seed regions. Seizure duration positively correlates with RSFC between parahippocampal gyri and the PCC but negatively correlates with connectivity between the PCC and frontal lobe. The observed pattern of disruption provides evidence for integration- and segregation-type network abnormalities and supports aberrant network organization among people with IGE.

1. Introduction

Idiopathic generalized epilepsy (IGE) is characterized by widespread cortical hyperexcitability with myoclonic, absence or generalized tonic–clonic seizures [1]. People with IGE do not exhibit abnormal brain anatomy or an identified focus of seizure activity but rather, widespread atypical cortical activity typified by generalized spike-and-wave discharges and seizures. Deviant neuronal activity stems from aberrant thalamo-cortical or cortico-cortical interactions that spread throughout the brain [2]. Abnormal neuronal activity at a distinct anatomic location that is part of a larger cortical network may be the basis for rapid propagation of aberrant neuronal firing that contributes to generalized seizures.

Distant neuronal assemblies that fire synchronously at very low frequencies maintain large-scale networks throughout the brain [3]. These low-frequency oscillations are identified by spontaneous increases in the blood oxygen level dependent (BOLD) signal on functional MRI (fMRI) at 0.01–0.1 Hz while the brain is at "rest" or not engaged in cognitive demands or goal-directed tasks [4]. Metabolic demands of the brain during active engagement only increase slightly over the rest condition, and several distinct regions of the

brain are noted to *decrease* in activity during tasks [5–7]. These areas, together termed the default mode network (DMN), are composed of the precuneus/posterior cingulate cortex (PCC), medial prefrontal cortex (MPFC), lateral parietal cortex and inferior temporal cortex and have been the focus of much investigation in recent years [8–10]. The nodes of this network spontaneously but synchronously show increases in the BOLD signal on fMRI, which give rise to the resting state functional connectivity (RSFC) of neuronal assemblies that show temporal coherence [11].

The DMN is referred to as the 'task-negative' network because its nodes show *decreased* activity during specific cognitive demands while the 'task-positive' network, composed of the dorsolateral prefrontal cortex, inferior parietal cortex and supplementary motor area, shows *increased* activity in response preparation [12,13]. Though the alternating synchrony of the spontaneous activity of these two networks suggests that they must be organized in some manner into one well-orchestrated unit, we refer to functional *integration* as temporally correlated activity in distinct nodes while *segregation* is the network of regions in which the time series of activation is anti-correlated [14]. The organization of the integration and segregation is well-preserved in healthy individuals but has been shown to break down in some neurological populations.

Healthy individuals reliably exhibit robust, positive correlations between regions of the DMN and negative correlations between DMN regions and other cortical areas. Abnormal DMN functional

* Corresponding author at: Department of Neurology, 423 East 23 St, #17087c, New York, NY 10016, USA.
E-mail address: thomas.thesen@med.nyu.edu (T. Thesen).

connectivity occurs in several brain disorders, including Alzheimer's disease [15], schizophrenia [16], ADHD [17], Parkinson's [18], and depression [19]. Decreased functional connectivity within the DMN has also been found in people with temporal lobe epilepsy [20]. There is conflicting evidence that people with IGE show differences in resting state functional connectivity (RSFC). Both Luo et al. and Song et al. demonstrated decreases in DMN integration in people with absence and general tonic–clonic epilepsy, respectively [21,22]. However, Moeller et al. showed no differences in functional connectivity in areas that deactivate the most during general spike-and-wave discharges, including nodes of the DMN [23]. Given the spontaneous, deviant neuronal activity that spreads throughout the brain in people with IGE, we aim to identify abnormal regions in the DMN and the extent to which these pathologic areas are a part of a larger network. We predict disruptions of the default mode network in the frontal lobes, consistent with previous studies showing frontal lobe abnormalities in IGE [24].

2. Methods

2.1. Participants

Fifteen people with IGE were recruited from the patient population at New York University Medical Center, Comprehensive Epilepsy Center (8 women, age range 20–48, mean age 30.13) and were age- and sex-matched with 15 healthy control subjects recruited from the general population (8 women, age range 21–43, mean age 29.8). Patients met criteria for IGE and had to have a history of seizures with no history of developmental delay or structural brain abnormalities. Standard, diagnostic structural imaging studies were normal. Electrophysiologic evaluation with interictal, and in most patients, ictal EEG demonstrated typical generalized epileptiform spikes; patients with focal epileptiform discharges or focal slowing on EEG were not eligible. People with IGE were classified according to the International League Against Epilepsy (ILAE) classification as having juvenile myoclonic epilepsy (JME) (40%), absence seizures (40%), unspecified myoclonic seizures (60%) or general tonic–clonic seizures (93%) (Table 1). All people diagnosed with IGE were under medical treatment at the time of study. All subjects gave their written informed consent to participate in this study, which was approved by the Institutional Review Board of NYU Langone School of Medicine.

2.2. Data acquisition

Functional MRI data were acquired on a Siemens Allegra 3.0 T scanner. We collected 197 contiguous echo planar imaging functional volumes for each subject (TR = 2000 ms; TE = 25 ms; flip angle = 90, 39 slices, matrix = 64×64; FOV = 192 mm; acquisition voxel size = 3×3×3 mm). All participants were instructed to lie as still as possible with their eyes closed for the duration of the 6-min, 38-second scan. A T1-weighted anatomical image was also acquired for spatial normalization and localization using a magnetization prepared gradient echo sequence (TR = 2530 ms; TE = 3.25 ms; T1 = 1100 ms; flip angle = 7; 176 slices; FOV = 256 mm).

2.3. fMRI data preprocessing

AFNI [25] was used to perform slice timing correction, motion correction, and detection and reduction of extreme time series outliers. The first 5 volumes of each participant's scan were discarded. All other data processing was done with FSL (FMRIB Software Library; www.fmrib.ox.ac.uk). Further processing included spatial smoothing using a Gaussian kernel (FWHM = 6 mm), mean-based intensity normalization (each subject's 4-D dataset was scaled by its global mean), and temporal bandpass filtering (0.01–0.1 Hz). To control for the effects of motion, as well as normal physiologic processes such as cardiac and respiratory rhythms, each participant's 4-dimensional (4-D) preprocessed volume was regressed on 9 predictors that modeled nuisance signals from white matter, cerebrospinal fluid and the global signal and 6 motion parameters. Correction for time series autocorrelation (prewhitening) was performed. Each voxel's time series was then scaled by its standard deviation, and the volume was spatially normalized to MNI152 standard space using linear registration. These methods were described in detail elsewhere [26].

2.4. DMN identification with anatomically distinct regions

Spherical seed regions of interest (ROIs) with radii of 6 mm were placed in areas consistently implicated in the DMN: the PCC (BA 31) and MPFC (BA 10), centered at MNI coordinates x = 3, y = −57, z = 26 (PCC) and x = 8, y = 59, z = 19 (MPFC) [9]. Although there are many distinct nodes in the DMN, these two structures were chosen as seed regions because they robustly elicit DMN maps, are not lateralized, and are distant anatomic regions that belong to a well-

Table 1
Patient characteristics.

Patient	Gender	Absence	Myoclonic	JME	Convulsion	Onset age	Age at MRI	AEDs
1	M	X	X		X	4	26	TPM
2	F	X	X		X	17[a]	48	LTG
3	M		X	X		20	27	LEV
4	F				X	19	32	LEV
5	F		X	X	X	13	22	LEV, LTG
6	F	X			X	18[a]	21	ETX, LTG
7	F				X	13	39	LEV, LTG, RUF, TPM
8	M	X	X		X	2	27	CBZ, VPA
9	M				X	9	35	LEV
10	M				X	31	36	VPA
11	M		X	X	X	12	25	OXC, ZNG
12	F	X	X	X	X	15	24	CLZ, LTG
13	M				X	15	20	LEV, TPM, VPA
14	F		X	X	X	14	37	CLZ, LEV
15	F	X	X	X	X	10	27	TPM

CBZ = carbamazepine, ETX = ethosuximide, CLZ = clonazepam, LEV = levetiracetam, LTG = lamotrigine, OXC = oxcarbazepine, RUF = rufinamide, TPM = topiramate, VPA = valproic acid, and ZNG = zonisamide.

[a] Patients were diagnosed with IGE based on scalp EEG and presentation to a hospital after first general tonic–clonic convulsion. It is unclear, though possible, that they experienced staring spells that would be consistent with absence epilepsy prior to this age of diagnosis. They did show clinical evidence of absence seizures after onset age, which were captured on video EEG.

characterized network [14]. The mean time series of each seed was obtained by applying these seed ROIs to each participant's 4-D residual standard space volume and averaging across the time series of each voxel within the ROI (see Fig. 1A). Subject-level RSFC maps of all voxels that were positively and negatively correlated with the seed ROI were generated by regressing each participant's 4-D residual volume on the seeds' time series. Group level RSFC analyses were carried out using an ordinary least squares model implemented in FSL, which generated Z-score maps ("networks") of positive and negative RSFC for each seed. Correlation coefficients of each voxel were normalized to Z-scores with Fisher's r-to-Z transformation. Maps of correlated networks were thresholded at $Z > 2.3$ and were corrected for multiple comparisons with a FDR criterion cluster level significance of $p < 0.05$.

2.5. Differences in DMN functional connectivity

To examine differences between positively and negatively correlated networks with the seed regions, a direct voxel-wise comparison was performed using a mixed-effects ordinary least squares model implemented in FSL, thresholded at $Z > 2.3$. Group difference maps were generated using both the PCC and MPFC seeds. Individual parameter estimates for each participant were generated for degree of correlation between the average time series in the voxels comprising the seed and all voxels included in the group difference ROI. This was done for each seed region and plotted with average values and standard error of the mean calculated.

Finally, to fully characterize all the brain regions showing a difference in connectivity with the abnormally integrated region elicited in the previous analysis, a 4-mm seed was centered on the point of maximum difference in connectivity. Using the mixed-effect ordinary

least squares model, a direct voxel-wise comparison between the people with IGE and healthy controls was performed.

2.6. Correlation analysis

The effects of seizure duration, age of seizure onset and age at time of scan on RSFC were examined by using these measures as covariates of positive and negative connectivity with each of the seeds. Seizure duration is defined as the time in years from first seizure to time of scan. With each of these measures used as regression coefficients implemented in FSL's general linear model, maps were generated that show clusters that co-vary positively and negatively with RSFC of both the PCC and MPFC seeds. The parameter estimates between the clusters elicited and seed voxels were correlated with each parameter mentioned above to determine the correlation coefficient.

3. Results

3.1. Integrated and segregated networks with MPFC and PCC seeds

Connectivity maps for each group and for each node of the DMN were generated. Both groups exhibited functional connectivity within areas of the DMN. Regions exhibiting positive RSFC with the MPFC seed in both groups included medial prefrontal cortex, extending to the paracingulate gyrus, superior frontal gyrus, middle frontal gyrus (superiorly and laterally), ventral ACC, precuneus/PCC, angular gyrus extending to the lateral occipital cortex, and middle temporal gyrus. In both groups, negative correlations were observed in the supramarginal gyrus extending to the superior occipital cortex and insular cortex. However, there were differences seen between the groups on visual inspection. Healthy controls had greater negative correlations with the planum temporale extending to the parietal
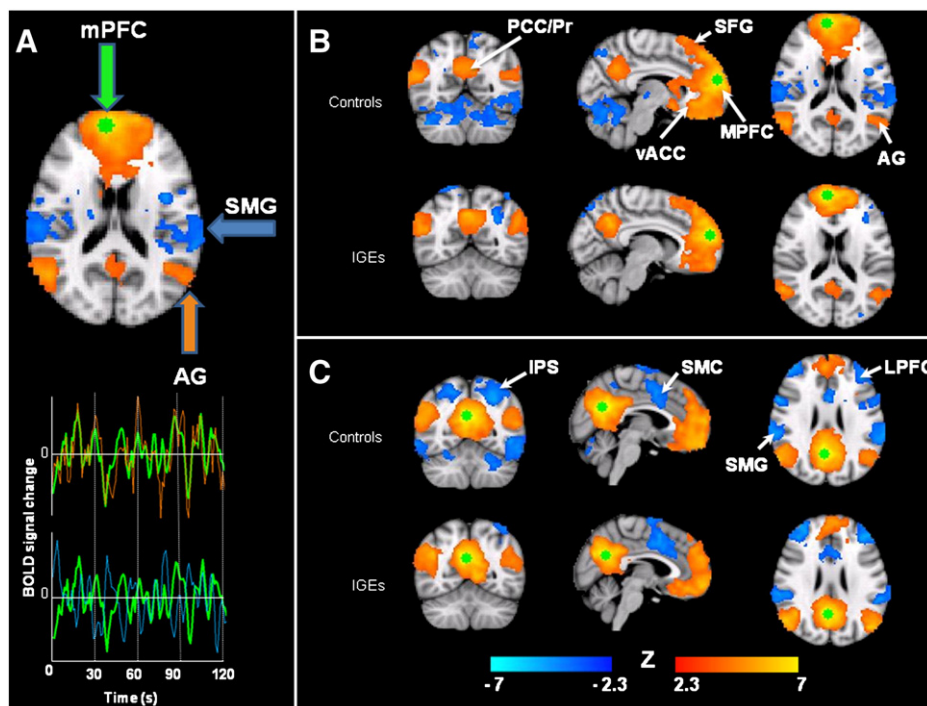

Fig. 1. Positively and negatively correlated time series with seed regions. A. Voxel-wise correlation map in a single control subject with a seed region in medial prefrontal cortex (MPFC) indicated by the circle in green. Brain regions in orange/yellow, such as the angular gyrus (AG), are positively correlated with the seed region, and brain regions in blue, such as the supramarginal gyrus (SMG) are anti-correlated with the seed region. Time courses of the average BOLD signal from the seed region (green trace), positively correlated AG (orange trace) and negatively correlated SMG (blue trace) are shown below. B. Red/yellow colors show brain regions that are positively correlated with the seed ROI (green circle) in the MPFC in controls and people with IGE. Blue colors show areas that are negatively correlated. C. Areas positively and negatively correlated with the seed in the PCC are shown in controls and people with IGE. PCC/Pr, posterior cingulate cortex/precuneus; vACC, ventral anterior cingulate cortex; SFG, superior frontal gyrus; MPFC, medial prefrontal cortex; AG, angular gyrus; IPS, intraparietal sulcus; SMC, supplementary motor cortex; SMG, supramarginal gyrus; and LPFC, lateral prefrontal cortex.

operculum, the lateral edge of the thalamus on the right and areas in the cerebellum (Fig. 1B).

Fig. 1C shows the areas positively and negatively correlated with the seed placed in the PCC in healthy control subjects and in people with IGE. Regions exhibiting positive RSFC with the PCC in both healthy controls and people with IGE included proximal areas of PCC and precuneus, angular gyrus, MPFC, ACC, paracingulate gyrus, and inferior temporal poles extending to the middle temporal gyrus. In both groups, negative correlations were observed in dorsolateral prefrontal cortex, insular cortex, planum polare, supramarginal gyrus, left intraparietal sulcus and dorsal anterior cingulate extending to the supplementary motor cortex. People with IGE failed to show negative correlations in the precentral gyrus, extending rostrally to the superior frontal gyrus and paracingulate gyrus, central opercular cortex, posterior inferior temporal gyrus, antero-superior aspects of the temporal lobe, left precentral gyrus, and cerebellum.

3.2. Direct group comparisons of RSFC

The direct comparison functional connectivity that was cluster-based thresholded at Z > 2.3 to control for false discovery rates between controls and people with IGE identified a group difference in the integrated network between each of the seeds in the PCC and MPFC and a cluster elicited more ventrally in the MPFC (Fig. 2). This area is consistently shown to be integrated in the DMN, but people with IGE lacked extensive positive RSFC in this area of the DMN compared to healthy controls and failed to show strong positive correlations (mean r = 0.07, SEM 0.02) compared to controls (mean r = 0.29, SEM 0.04). Similarly, DMN connectivity based on the seed in the MPFC exhibited a group difference within the same area of the prefrontal cortex. People with IGE did not reliably show strong positive correlations between these areas (IGE group mean r = 0.22, SEM 0.03; control group mean r = 0.41, SEM 0.03). Scatter plots in both panels of Fig. 2 show the correlation values for each participant.

To further examine the group differences in RSFC in prefrontal cortex areas, we performed an additional analysis to investigate the connectivity network of the discordant region in the prefrontal cortex seen in warm colors in Fig. 2. A seed with a radius of 4 mm was placed where differences in PCC RSFC between controls and people with IGE were maximal in the prefrontal cortex cluster at MNI coordinates −2, 44, 0 (Fig. 3). The difference from the PCC RSFC was the most robust though the point of maximal difference elicited from the MPFC seed was adjacent. Maps of significant group differences in RSFC were generated in the same manner as for the primary PCC and MPFC seed analyses. The comparison map (healthy controls v. people with IGE) thresholded at Z > 2.3 and corrected for multiple comparisons showed robust group differences in both positive and negative RSFC between the disrupted node in the prefrontal cortex and areas typically integrated in the DMN and segregated from the DMN. Specifically, patients did not consistently show positive correlations with areas included in the 'task-negative' network, namely the dorsal–medial prefrontal cortex, extending from the superior frontal gyrus to the paracingulate gyrus and ventral ACC, and the PCC/precuneus (control group mean r = 0.20, SEM = 0.02 IGE group mean r = 0.01, SEM = 0.02). Group differences also appeared in areas typically negatively correlated with the DMN, in the 'task-positive' network. All controls showed negative correlations between the seed in the PFC and the areas shown in blue on the group difference map, such as the supramarginal gyrus, superior parietal lobule, and intraparietal sulcus, while the majority of IGE patients showed positive correlations between these areas (control group r = −0.15, SEM 0.02; IGE group r = 0.02, SEM 0.01). Scatter plots show that all healthy controls exhibit positive RSFC between the seed in the PFC (green) and areas typically integrated in the DMN (red) while people with IGE exhibit overall decreased or negative functional connectivity between these areas. Similarly, the negative connectivity scatter plot illustrates that healthy controls consistently show negative RSFC between the seed and areas in the task-negative network (blue) though our cohort of people with epilepsy fail to show strong segregation in these areas.
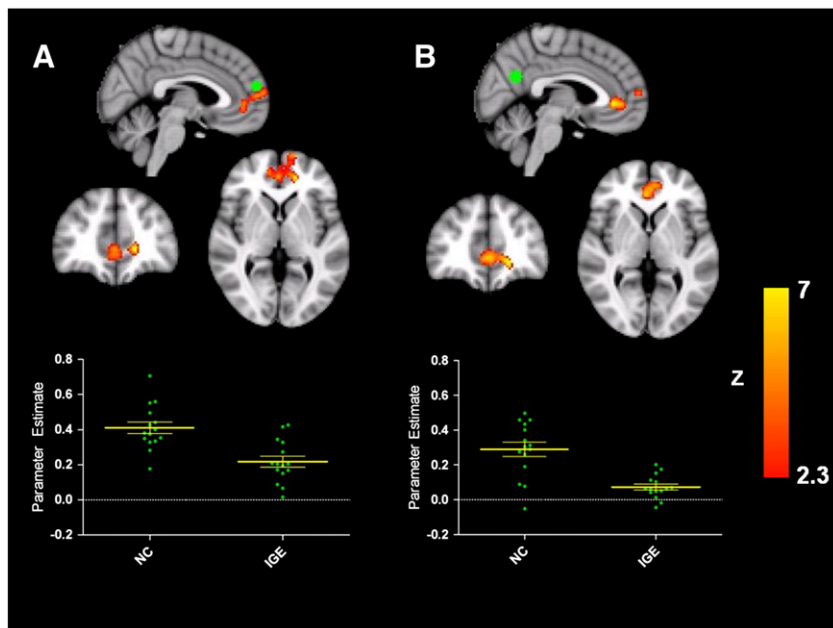

Fig. 2. Group differences in functional connectivity between patients and controls. The cortical cluster shown in red in both panels is the cluster that exhibits group differences between healthy controls and people with IGE upon direct comparison with cluster-based thresholding at Z > 2.3. Both differences between the functional connectivity of the seed regions in the MPFC (A) and the posterior cingulate cortex (PCC) (B) show differences in the same prefrontal cortex region (red cluster in both A and B). Scatter plots show the parameter estimate or correlation of the low-frequency oscillations of the BOLD signal between the seed regions and the entire ROI (red) in the prefrontal cortex. The scatter plot in (A) shows that healthy controls (NC) tend to show stronger correlations in resting state functional connectivity (RSFC) between both the MPFC seed (green) and the PFC cluster (red). Similarly, the scatter plot in (B) shows that NC subjects have greater RSFC between the PCC seed (green) and PFC (red) than people with IGE.
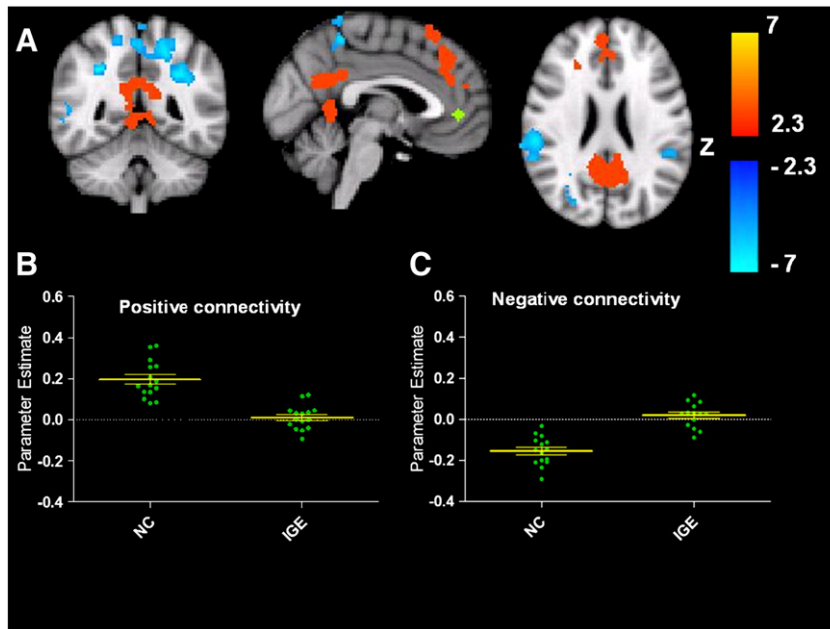
Fig. 3. Group differences in functional connectivity from abnormal region in the prefrontal cortex. A. When a seed was placed in the abnormal PFC region (green), the cortical maps of group differences upon direct comparison with cluster-based thresholding at Z>2.3 show that healthy controls exhibit greater positive RSFC than people with IGE in areas typically included in the DMN (red areas) and greater negative RSFC in areas typically included in the 'task-positive' networks (blue areas). B. The scatter plot shows the degree of RSFC (the parameter estimate) between the green seed region and all red clusters in both the healthy controls (NC) and people with IGE. C. The scatter plot shows the parameter estimate of the green seed region and all blue clusters in NC and IGE. Yellow bars show the mean and standard error of the mean in each plot.

3.3. Correlation analyses

When parameters such as seizure onset age, age at time of scan and seizure duration were used as regressors with the correlation analysis for functional connectivity of both the PCC and MPFC seeds, only seizure duration correlated with network differences from the PCC node (Fig. 4). Seizure duration was positively correlated with increased RSFC between the PCC and bilateral anterior temporal lobes, primarily in the parahippocampal cortex ($R^2 = 0.71$, $p<0.005$). Seizure duration was also negatively correlated with decreased RSFC between the PCC and a cluster in the frontal cortex ($R^2 = 0.64$, $p<0.005$), dorsal to the cluster in the DMN that showed decreased
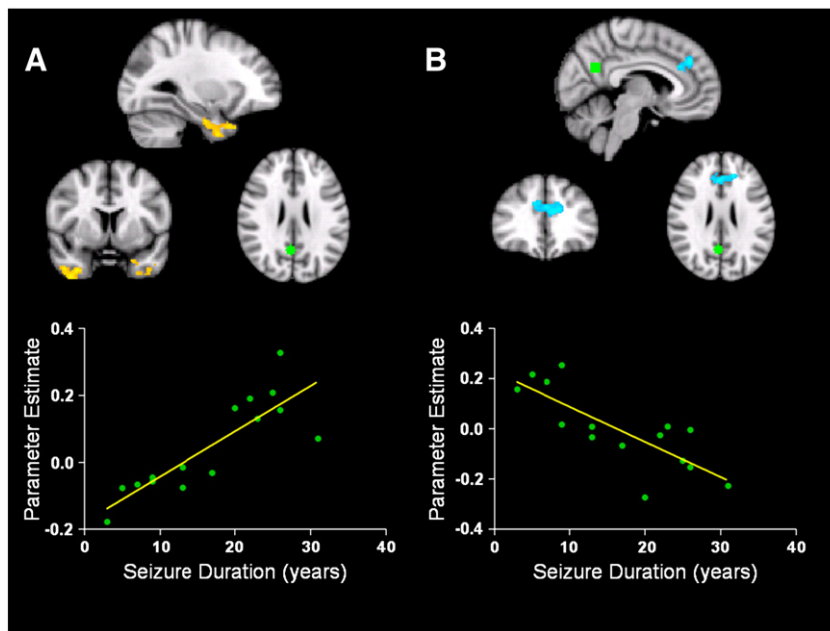

Fig. 4. Functional connectivity with PCC seed regressed with seizure duration. A. Seizure duration positively varies with the correlations between the average time series of the seed in the PCC (green) and clusters bilaterally in the anterior temporal lobes (yellow). The scatter plot shows the relationship between seizure duration and parameter estimates between the regions specified ($R^2 = 0.71$, $p<0.005$). B. Seizure duration negatively varies with the parameter estimates between the PCC and a cluster near the anterior cingulate cortex in the frontal lobe. The scatter plot shows the relationship between seizure duration and parameter estimates between the regions specified ($R^2 = 0.62$, $p<0.005$). Each green point on the scatter plots represents a person with IGE's RSFC between the seed and ROI and their seizure duration.

integration compared to controls (Fig. 4). These areas failed to show any correlation with onset age or age at time of scan. None of the parameters used as regressors showed any differences with network integration or segregation from the MPFC seed.

4. Discussion

Using R-fMRI, we examined the integrity of the DMN at rest in people with IGE and found abnormalities in interictal RSFC. Specifically, those with IGE have diminished RSFC between nodes of the DMN and a cluster in the PFC, relative to healthy controls. People with IGE exhibit both disrupted functional network *integration* (positive RSFC between nodes of the DMN) and functional *segregation* (negative RSFC between areas of the DMN and "task-positive" regions), supporting aberrant functional network organization in people with IGE.

4.1. Decreased positive functional connectivity in the frontal cortex

Collectively, the participants with IGE showed abnormal functional connectivity within the DMN. They exhibited decreased positive RSFC between areas in the frontal lobe and the rest of the DMN. These areas serve various cognitive and emotional functions, including "mentalizing" (i.e., understanding the mental states of one's self and others) [27–29]. Patients with IGE show difficulties in social processing similar to those exhibited by patients with frontal lobe lesions [30], including limited self-control, suggestibility, distractibility, and indifference to physical needs [31,32]. Such deficits may be the result of impaired mentalizing abilities such as concept formation, abstract reasoning, mental flexibility, cognitive speed and planning [33]. Furthermore, the cluster in the frontal lobe showed abnormal segregation from regions typically considered to be part of 'task-positive' network including lateral parietal and occipital regions. Though the cognitive implications of decreased *segregation* among these areas would be speculative, these group differences strengthen the argument that an abnormal area in the frontal cortex is neither well integrated into the default mode network nor segregated from task-positive networks. Future studies should investigate whether the decreased frontal DMN RSFC observed in this study is related to these IGE-related social-cognitive impairments.

Physiological recordings in rat models support our findings of frontal lobe dysfunction, where aberrant firing rates and patterns have been observed in MPFC neurons during spike-and-wave discharges [34]. Source localization utilizing MEG has identified frontal lobe localizations in people with IGE [35,36]. In people with juvenile myoclonic epilepsy, spike-and-slow wave discharges were modeled to the medial prefrontal region [35]. An EEG-fMRI study of a patient with IGE revealed frontal deactivation during a generalized spike-wave discharge [37]. These studies, together with our results, suggest that frontal deactivations may disrupt the DMN and contribute to the cognitive and behavioral deficits in IGE.

Differences in RSFC with the PCC that correlate with seizure duration are not limited to the MPFC and are specific to the PCC seed only. These abnormalities extend beyond the DMN, but we address them here because the PCC is a prominent node of the DMN. The frontal lobe cluster that shows decreased RSFC with the PCC seed negatively correlates with seizure duration. This suggests that the chronic effects of seizures, epileptiform activity, and the underlying abnormalities disrupt the functional integration between medial posterior and frontal regions. fMRI studies show negative BOLD responses (NBR) in frontal, parietal and posterior cingulate cortices during GSW discharges [38]. Surprisingly, we found seizure duration significantly correlated with increased connectivity of both parahippocampal gyri to the PCC seed. Though frontal–thalamic circuits are implicated in IGE, temporal lobe function may also be affected in generalized epilepsies. Frontal and temporal volumes are decreased in childhood

absence epilepsy [39], and perirhinal kindling increases discharges in a rat model of absence epilepsy [40]. Our finding of increased parahippocampal connectivity to the PCC seed may reflect either 1) increased synchronization of these limbic regions in people with IGE, 2) a disinhibition reflecting loss of frontal inhibitory input on this circuit, or 3) other processes.

IGE-related disruption in DMN RSFC may reflect chronic disorganization of the functional architecture due to neurophysiologic dysfunction (e.g., channelopathy) or intermittent disruptions to that functional architecture that perturbs cortical networks (e.g., frequent abnormal discharges). Differences between the RSFC of a region in the PFC to the DMN and task-positive areas suggest that the disruptions affect the DMN as well as extensive cortical networks. Further work combining R-fMRI with electrophysiological recordings providing access to high-frequency neuronal signals may help adjudicate between these alternatives.

4.2. Limitations and future directions

In our study, healthy subjects expectedly and uniformly showed either strong positive or negative correlations within the DMN. In turn, people with IGE showed both a decrease and greater variability in connectivity strength, potentially identifying a feature of the population or a potential effect of other disease-related variables. As this study utilized a cross-sectional sample of controls as well as patients, it is not known whether the network differences we found manifested before seizure onset, or result from seizures, medications, spike-and-wave discharges, and other disease-related factors. Longitudinal studies would confirm that seizure duration correlates with changes in DMN RSFC over time. Future studies should use simultaneous EEG-fMRI to determine whether periodic epileptiform discharges contribute to the observed group differences in DMN functional connectivity. Further studies would also benefit from investigating the relationship of the specific cognitive deficits seen in this patient population and its relation to DMN integrity.

Conflict of interest statement

None of the authors has any conflicts of interest to disclose. We confirm that we have read the journal's position on issues involved in ethical publication and affirm that this report is consistent with those guidelines.

Acknowledgements

References

[1] Gloor P. Generalized epilepsy with bilateral synchronous spike and wave discharge. New findings concerning its physiological mechanisms. Electroencephalogr Clin Neurophysiol Suppl 1978:245–9.
[2] Tyvaert L, Chassagnon S, Sadikot A, LeVan P, Dubeau F, Gotman J. Thalamic nuclei activity in idiopathic generalized epilepsy: an EEG-fMRI study. Neurology 2009;73:2018–22.
[3] Buzsaki G, Draguhn A. Neuronal oscillations in cortical networks. Science 2004;304:7709–17.
[4] Biswal B, Yetkin FZ, Haughton VM, Hyde JS. Functional connectivity in the motor cortex of resting human brain using echo-planar MRI. Magn Reson Med 1995;34:537–41.
[5] Raichle ME, MacLeod AM, Snyder AZ, Powers WJ, Gusnard DA, Shulman GL. A default mode of brain function. Proc Natl Acad Sci 2001;98:676–82.
[6] Esposito F, Bertolino A, Scarabino T, et al. Independent component model of the default-mode brain function: assessing the impact of active thinking. Brain Res Bull 2006;70:263–9.
[7] Fransson P. Spontaneous low-frequency BOLD signal fluctuations: an fMRI investigation of the resting-state default mode of brain function hypothesis. Hum Brain Mapp 2005;26:15–29.

[8] Greicius MD, Krasnow B, Reiss AL, Menon V. Functional connectivity in the resting brain: a network analysis of the default mode hypothesis. Proc Natl Acad Sci U S A 2003;100:253–8.

[9] Uddin LQ, Kelly AM, Biswal BB, Castellanos FX, Milham MP. Functional connectivity of default mode network components: correlation, anticorrelation, and causality. Hum Brain Mapp 2009;30:625–37.

[10] Raichle ME, Snyder AZ. A default mode of brain function: a brief history of an evolving idea. Neuroimage 2007;37:1083–90.

[11] Friston KJ. Functional and effective connectivity in neuroimaging: a synthesis. Hum Brain Mapp 1994;2:56–78.

[12] Fox MD, Snyder AZ, Vincent JL, Corbetta M, Van Essen DC, Raichle ME. The human brain is intrinsically organized into dynamic, anticorrelated functional networks. Proc Natl Acad Sci U S A 2005;102:9673–8.

[13] Sonuga-Barke EJS, Castellanos FX. Spontaneous attentional fluctuations in impaired states and pathological conditions: a neurobiological hypothesis. Neurosci Biobehav Rev 2007;31:977–86.

[14] Fair DA, Dosenbach NU, Church JA, et al. Development of distinct control networks through segregation and integration. Proc Natl Acad Sci U S A 2007;104: 13507–12.

[15] Greicius MD, Srivastava G, Reiss AL, Menon V. Default-mode network activity distinguishes Alzheimer's disease from healthy aging: evidence from functional MRI. Proc Natl Acad Sci U S A 2004;101:4637–42.

[16] Garrity AG, Pearlson GD, McKiernan K, Lloyd D, Kiehl KA, Calhoun VD. Aberrant "default mode" functional connectivity in schizophrenia. Am J Psychiatry 2007;164: 450–7.

[17] Tian L, Jiang T, Wang Y, et al. Altered resting-state functional connectivity patterns of anterior cingulate cortex in adolescents with attention deficit hyperactivity disorder. Neurosci Lett 2006;400:39–43.

[18] Van Eimeren T, Monchi O, Ballanger B, Strafella AP. Dysfunction of the default mode network in Parkinson disease: a functional magnetic resonance imaging study. Arch Neurol 2009;66:877–83.

[19] Greicius MD, Florew BH, Menon V, et al. Resting-state functional connectivity in major depression: abnormally increased contributions from subgenual cingulate cortex and thalamus. Biol Psychiatry 2007;62:429–37.

[20] Zhang Z, Lu G, Zhong Y, et al. Altered spontaneous neuronal activity of the default-mode network in mesial temporal lobe epilepsy. Brain Res 2010;1323: 152–60.

[21] Luo C, Li Q, Lai Y, et al. Altered functional connectivity in default mode network in absence epilepsy: a resting-state fMRI study. Hum Brain Mapp 2011;32:438–49.

[22] Song M, Du H, Wu N, et al. Impaired resting-state functional integrations within default mode network of generalized tonic–clonic seizures epilepsy. PLoS One 2011;6(2):e17294.

[23] Moeller F, Maneshi M, Pittau F, et al. Functional connectivity in patients with idiopathic generalized epilepsy. Epilepsia 2011;52(3):515–22.

[24] Holmes MD, Brown M, Tucker DM. Are "generalized" seizures truly generalized? Evidence of localized mesial frontal and frontopolar discharges in absence. Epilepsia 2004;45:1568–79.

[25] Cox RW. AFNI: software for analysis and visualization of functional magnetic resonance neuroimages. Comput Biomed Res 1996;29:162–73.

[26] Kelly C, De Zubicaray G, Di Martino A, et al. L-dopa modulates functional connectivity in striatal cognitive and motor networks: a double-blind placebo-controlled study. J Neurosci 2009;29:7364–78.

[27] Gusnard DA, Akbudak E, Shulman GL, Raichle ME. Medial prefrontal cortex and self-referential mental activity: relation to a default mode of brain function. Proc Natl Acad Sci U S A 2001;98:4259–64.

[28] Simpson JR, Drevets WC, Snyder AZ, Gusnard DA, Raichle ME. Emotion-induced changes in human medial prefrontal cortex: II. During anticipatory anxiety. Proc Natl Acad Sci U S A 2001;98:688–93.

[29] Amodio DM, Frith CD. Meeting of minds: the medial frontal cortex and social cognition. Nat Rev Neurosci 2006;7:268–77.

[30] Damasio H, Grabowski T, Frank R, Galaburda AM, Damasio AR. The return of Phineas Gage: clues about the brain from the skull of a famous patient. Science 1994;264:1102–5.

[31] Bech P, Pedersen K, Simonsen N, Lund M. A multidimensional study of personality traits ad modum Sjobring. Acta Neurol Scand 1976;54:348–58.

[32] De Araujo Filho GM, Jackowski AP, Lin K, et al. Personality traits related to juvenile myoclonic epilepsy: MRI reveals prefrontal abnormalities through a voxel-based morphometry study. Epilepsy Behav 2009;15:202–7.

[33] Devinsky O, Gershengorn J, Brown E, Perrine K, Vazquez B, Luciano D. Frontal functions in juvenile myoclonic epilepsy. Neuropsychiatry Neuropsychol Behav Neurol 1997;10:243–6.

[34] Lorincz M, Olah M, Baracskay P, Szilagyi N, Jhuasz G. Propagation of spike and wave activity to the medial prefrontal cortex and dorsal raphe nucleus of WAG/Rij rats. Physiol Behav 2007;90:318–24.

[35] Santiago-Rodriguez E, Harmony T, Fernandez-Bouzas A, et al. Source analysis of polyspike and wave complexes in juvenile myoclonic epilepsy. Seizure 2002;11:320–4.

[36] Stefan H, Paulini-Ruf A, Hopfengartner R, Rampp S. Network characteristics of idiopathic generalized epilepsies in combined MEG/EEG. Epilepsy Res 2009;85:187–98.

[37] Laufs H, Lengler U, Hamandi K, Kleinschimdt A, Krakow K. Linking generalized spike-and-wave discharges and resting state brain activity by using EEG/fMRI in a patient with absence seizures. Epilepsia 2006;47:444–8.

[38] Hamandi K, Laufs H, Noth U, Carmichael DW, Duncan JS, Lemieux L. BOLD and perfusion changes during epileptic generalized spike wave activity. Neuroimage 2008;39:608–18.

[39] Caplan R, Levitt J, Siddarth P, et al. Frontal and temporal volumes in childhood absence epilepsy. Epilepsia 2009;50(11):2466–72.

[40] Ackman O, Karson A, Aker RG, Ates N, Onat FY. Perirhinal cortical kindling in rats with genetic absence epilepsy. Neurosci Lett 2010;479:74–8.